

INTERFEROMETRIC MONITORING OF AN ACTIVE UNDERGROUND MINING FIELD WITH HIGH-RESOLUTION SAR SENSORS

D. Walter^{a,*}, U. Wegmüller^b, V. Spreckels^c, W. Hannemann^a, W. Busch^a

^a TU Clausthal, Institute of Geotechnical Engineering and Mine Surveying, Erzstr. 18, D-38678 Clausthal-Zellerfeld, Germany – (diana.walter, wilhelm.hannemann, wolfgang.busch)@tu-clausthal.de

^b GAMMA Remote Sensing AG, Worbstr. 225, CH-3073 Gümligen, Switzerland – wegmuller@gamma-rs.ch

^c RAG Deutsche Steinkohle, Dept. BG G, Shamrockring 1, D-44623 Herne, Germany – volker.spreckels@rag.de

KEY WORDS: Radar, SAR Interferometry, GIS, Monitoring, Surface, High resolution, Accuracy Analysis, Terrain Motion

ABSTRACT:

Underground mining activities lead to ground movements at the earth surface. An area-wide monitoring and the documentation of mining induced influences are required by the mining authorities. Work done in the past confirmed a significant potential of SAR interferometric methods to contribute information to such monitoring. Nevertheless, in spite of advanced SAR interferometric processing techniques and numerous convincing results, there are general limitations to the utility of the application. For the monitoring of mining induced deformation information gaps may occur, especially in the case of high deformation rates. Another common problem of SAR interferometry is the loss of coherence in rural areas. The new generation of SAR sensors shows a significant improvement of the applicability of interferometric techniques for mining related surface deformation. The higher spatial resolution of the TerraSAR-X sensor and its shorter repeat intervals lead to easier phase unwrapping with the possibility to measure high deformation rates. Alternatively, the use of the longer L-band wavelength of ALOS PALSAR offers good possibilities in rural areas and in the case of fast surface movements.

The German hard coal mining company RAG Aktiengesellschaft (RAG), in cooperation with the Clausthal University of Technology and GAMMA Remote Sensing set up the R&D project “GeoMon” to investigate the potential of the available new SAR sensors for monitoring surface deformations above an active and an abandoned mine. The results of the interferometric analysis using TerraSAR-X and ALOS PALSAR data will be presented combined with the validation of the results with comprehensive terrestrial measurements.

1. INTRODUCTION

The successful launches of the satellites ALOS (L-band) and TerraSAR-X (X-band) have made available high-resolution SAR images with high potential for ground motion monitoring. Previously, the use of C-band SAR sensors showed limitation for deformation monitoring in rural areas and in the case of high deformation rates and gradients. The higher spatial resolution of the TerraSAR-X sensor and its shorter repeat intervals lead to easier phase unwrapping with the possibility to measure high deformation rates. Alternatively, the use of the longer L-band wavelength of ALOS PALSAR offers good possibilities in rural areas and in the case of fast surface movements.

Underground mining activities lead to ground motions at the earth surface. A regular area-wide monitoring and the documentation of mining influences are required in Germany by the mining authorities. Currently, there is a high interest in the mining sector in SAR interferometric techniques. But it is not clarified whether these techniques are able to contribute to the fulfilment of legal requirements by the mining industries as well as by the federal mining authorities.

RAG started research projects to evaluate SAR interferometric techniques and the potential of the available new SAR sensors TerraSAR-X and ALOS PALSAR also in comparison to ENVISAT ASAR for monitoring surface deformations above an active and abandoned underground mine. For these purposes RAG developed a monitoring concept in cooperation with

Clausthal University of Technology based on terrestrial measurements and simultaneous SAR sensor recordings. Furthermore, artificial corner reflectors were installed and in-situ measurements were collected.

2. DATA SELECTION

The investigation area is located in the Ruhr region of Germany. Active and abandoned mining fields are located in this rural district with small cities.

For interferometric monitoring were used data of following satellites (sensor, repeat-cycle, ground resolution, incidence angle, wavelength, number of scenes):

- TerraSAR-X (StripMap Mode, 11 (max. 33) days, 2.1m x 1.9m, 41°, $\lambda = 3.1\text{cm}$, #23 since 02/2008)
- ALOS (PALSAR – FBS, FBD, 46 (max. 230) days, 7.5 x 3.1m, 39°, $\lambda = 23.6\text{cm}$, #8+6 since 01/2007)
- ENVISAT (ASAR, 35 (max. 105) days, 20m x 4m, 23°, $\lambda = 5.6\text{cm}$, #49 since 12/2003)

PALSAR data were provided for two different tracks.

More details on the used data are described in (Walter et al., 2008; Wegmüller et al. 2008).

Each one of the used sensors operates in a different frequency band, has a different ground resolution (Fig. 1) and sensitivity

* Corresponding author.

against ground deformations, atmosphere and vegetation. The PALSAR sensor is suited for monitoring of high and fast motions, also in rural areas because of his long wavelength. TerraSAR-X is very sensitive against small and slow deformations, but also against fast deformations with high gradients because of the repeat cycle of 11 days and high ground resolution. A disadvantage of TerraSAR-X is the highest influence of data by atmosphere.



Figure 1. Mean intensity images of different sensors (ENVISAT ASAR, ALOS PALSAR, TerraSAR-X) with different ground resolution

However, besides technical characteristics of sensors, aspects as life of satellite, future satellites, swath, costs, assurance and time of delivery for ordered scenes, quality of scene (baseline, atmosphere, vegetation) and so on playing an import role for future operational use of SAR interferometric monitoring in the mining sector. For example ALOS basic observation scenario did not allow to record PALSAR data at desired times. One barrier for the mining industry to commercially use TerraSAR-X data are actually the high data prices. These are only few examples of relevant factors for operational application of SAR data for deformation monitoring.

3. SAR PROCESSING

SAR processing was conducted using GAMMA software. The processing was started from raw data for ASAR and PALSAR and from SLC data for TerraSAR-X. Raw data were processed to SLC and then coregistered to the same slant-range geometry. We continued to work with a multilooking of 1x5 (ENVISAT), 1x2 (PALSAR) and 2x2 (TerraSAR-X). The standard deviation of co-registration was smaller than 0.2 pixel for each sensor (Tab. 1). Absolute accuracy of co-registration was determined with artificial pentagonal corner reflectors (CR). The peak position of CRs was observed in intensity images, but under condition that CRs were not affected by horizontal deformations.

sensor	standard deviation of co-registration (max)		maximum difference of CR peak position	
	range [m]	azimuth [m]	range [m]	azimuth [m]
ASAR	1.6m	0.7m	4.6m	0.8m
PALSAR	1.4m	0.6m	3.1m	0.7m
TerraSAR-X	0.2m	0.3m	0.2m	0.1m

Table 1. Maximum standard deviation of co-registration

For the processing of single interferometric data pairs, two-pass differential interferometry was applied using an external DEM for topographic phase correction. For PALSAR data, the methodology used for mixed FBS and FBD pairs is described in more detail in (Werner 2007).

For precise geocoding and the subtraction of the topographic phase the high resolution NEXTMap® DTM (*Intermap Technologies Inc.*) with a 5m grid and an accuracy of 1.0m in

position and height (RMSE) was used. Details on the geocoding are described in (Walter, 2008). Absolute accuracies of geocoding were determined by CR, which were installed in the mining area, aligned to all sensors and measured with GPS and levelling methods. Our investigations showed that absolute geocoding accuracy is depending on spatial resolution of used DEM. For a SRTM-C (3'') and SRTM-X (1'') DEM-mosaic absolute geocoding accuracies of about 25m to 40m in range and 10m to 15m in azimuth were achieved in our case for all sensors. These values were not satisfactory for the high resolution SAR data. The NEXTMap® DTM showed the possibility to reach an absolute geocoding accuracy of about 3m (Fig. 2)

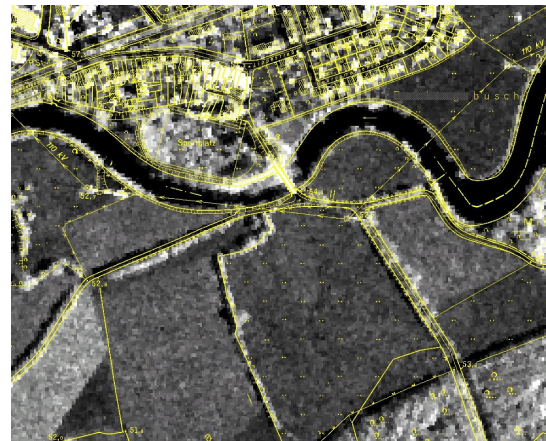


Figure 2. Examination of absolute geocoding accuracy of TerraSAR-X data with topographic map 1:5000

4. RESULTS

4.1 Differential SAR interferometry

All combinations of differential interferograms were calculated for every sensor. Analyses show that about 5% of all ENVISAT ASAR interferograms showed very good signal coherences over complete investigation area, but only for winter periods (Fig. 3). Maximum of about 45% of all interferograms showed only good coherences in urban areas. Causes for decorrelation were high temporal and spatial baselines, vegetation and too fast movements. This resulted in an incomplete detection of mining induced subsidence basins.

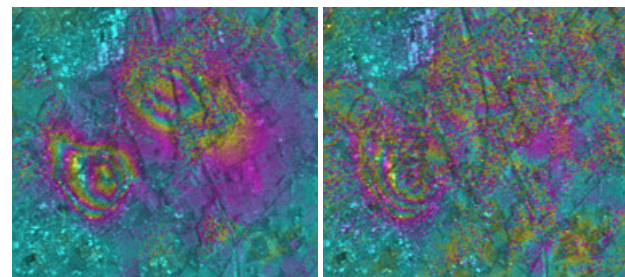


Figure 3. ENVISAT ASAR differential interferograms (70 days); left: 22/11/2007 – 31/01/2008 ($B_{\text{perp}}=2\text{m}$), right: 18/10/2007 – 27/12/2009 ($B_{\text{perp}}=253\text{m}$)

TerraSAR-X differential interferograms for winter periods showed very good coherences up to 33 days for rural and urban areas (Fig. 4). Forest areas showed total decorrelation for all times. Because of high sensitivity of X-band against changes of vegetation, decorrelation appeared in 11-days interferogram for

agriculture areas between spring and autumn. Geometric decorrelations couldn't be observed in TerraSAR-X interferograms, because of its high signal bandwidth. Regions with higher phase gradients and faster deformations showed clearly better coherences in TerraSAR-X images against ASAR. In contrast X-band signals were affected stronger by atmospheric delays in comparison with ASAR. For all differential interferograms an estimation and subtraction of the low frequency part of the phase was performed as atmospheric correction. The low frequency part had to be carefully determined because it was important to be aware of coexistent low frequency deformation.

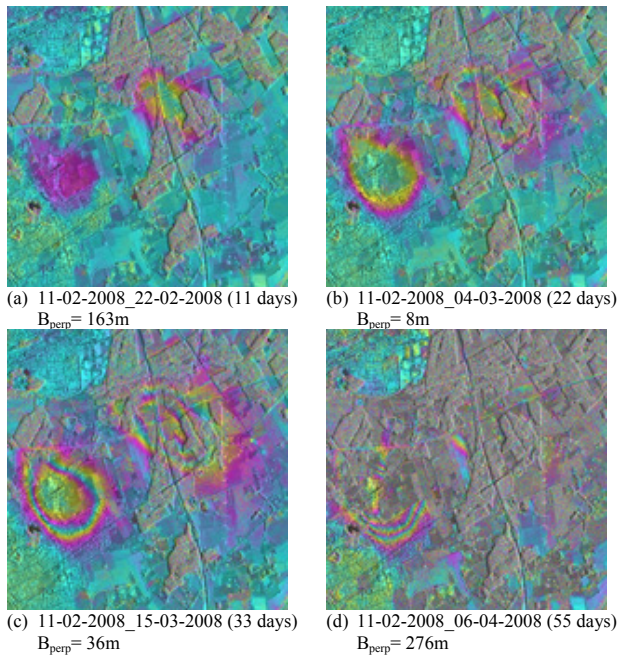


Figure 4. TerraSAR-X differential interferograms; vertical displacement = 2.06cm/fringe

East-west profiles (Fig. 5) through the western subsidence basin of Figure 4 show clearly the effect of advanced mining and the development of a symmetric to an asymmetric subsidence trough. The rate of subsidence has been doubled since 04-03-2008 in the centre of basin from about 10mm/11days to 20mm/11days.

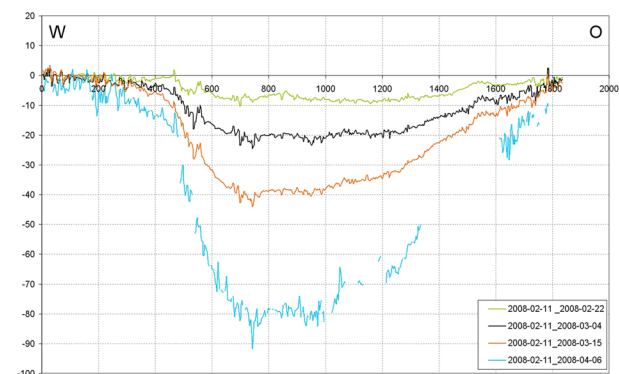


Figure 5. TerraSAR-X east-west profiles of subsidence basin [mm] for the same time periods of Figure 4

PALSAR differential interferograms in Figure 6 show that an almost complete spatial coverage with deformation information was achieved for 46 day intervals. In spite of the rural character

of test site and high deformation rates of about 10cm per month the differential interferograms showed very good coherences for the whole area, even after 4.5 month.

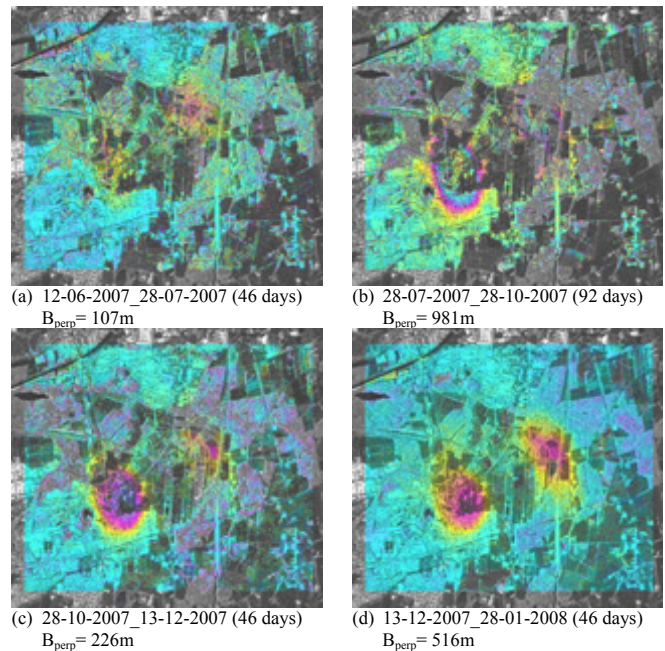


Figure 6. Unwrapped PALSAR differential interferograms; vertical displacement = 10cm/color cycle

The phase decorrelation in L-band interferograms appeared earlier for agriculture areas than for forest areas. The derivation of deformations was not possible for the differential interferogram with a perpendicular baseline B_{\perp} longer than 5.000m and a temporal baseline up to 7-8 month. The phase unwrapping of differential interferograms with baselines longer than 3.000m and scenes recorded in totally different seasons was difficult up to impossible. Figure 6 show time series of measured PALSAR deformations with in- and decreasing of the rate of motion.

NEXTMap terrain model, which is not equivalent to SAR scattering surface, was used for topographic correction. Because of this aspect, topographic phase errors appeared in differential interferograms. Misinterpretations of topographic fringes as deformation could result. TerraSAR-X differential interferograms showed a high sensitivity against topographic errors because of small wavelength und high resolution, like PALSAR differential interferograms because of their long baselines (Tab. 2).

sensor	θ_{inc}	perp. baseline [m]	height-to-phase factor [m/fringe]
ENVISAT ASAR	23°	100	92
		370	25
ALOS PALSAR	39°	500	131
		1000	65
		2600	25
TerraSAR-X	41°	50	138
		110	63
		280	25

Table 2. Height-to-phase factor for different perpendicular baselines of applied sensors with incidence angle θ_{inc}

4.2 Persistent scatterer results

Besides classical method of differential SAR interferometry, we used persistent scatterer interferometry (PSI) for determination

of deformations. The Interferometric Point Target Analysis (IPTA) is GAMMA's implementation of PSI. It is a method to exploit the temporal and spatial characteristics of interferometric signatures collected from point targets to accurately map surface deformation histories, terrain heights, and relative atmospheric path delays. The use of targets with point like scatter characteristics has the advantage that there is much less geometric decorrelation. More details to point target based interferometric technique used see (Wegmüller, 2004; Wegmüller, 2008).

PSI analysis was conducted with an ASAR data stack of 49 scenes and a TerraSAR-X data stack of 20 scenes. PSI with PALSAR data was impossible because of too few scenes.

The distribution of persistent scatterer points (PS) was very inhomogeneous over the mining area (Tab. 3). Due to the high-resolution TerraSAR-X data we got significantly more PS for urban areas in particular. PS were typical located at buildings, metallic surfaces and so on (Fig. 7).

Sensor	Rural area	Urban area	Mixed area	
	PS per km ²	PS per km ²	PS per km ²	PS in % of all SLC pixel
ASAR	20	330	88	0.7
TerraSAR-X	500	15000	3900	1.6

Table 3. Number of final persistent scatterer points of IPTA



Figure 7. TerraSAR-X persistent scatterer for urban area without deformation

In the result of PSI analysis we could identify and measure all subsidence basins above the mining fields. We could discover a before unknown area of minimal deformations above an abandoned mine from TerraSAR-X data as well as ASAR.

For regions with vegetation and high rates of deformations and non-uniform temporal gradients, we couldn't detect PS with ASAR (Fig. 9). To optimize the PSI processing of high-resolution TerraSAR-X data for the case of high deformation gradients and non-uniform motion, we worked with a multi-reference stack that included pairs with shorter time intervals (11- to 44-days) (see Wegmüller, 2008). In result a significant larger number of PS could be analysed for TerraSAR-X (Fig. 8). For agriculture and forest areas no PSI result was obtained. In comparison to dInSAR PSI had the important advantage to measure the complete temporal behaviour of the PS points every 11 days. On the other hand with dInSAR we only derived deformation results for individual time intervals.

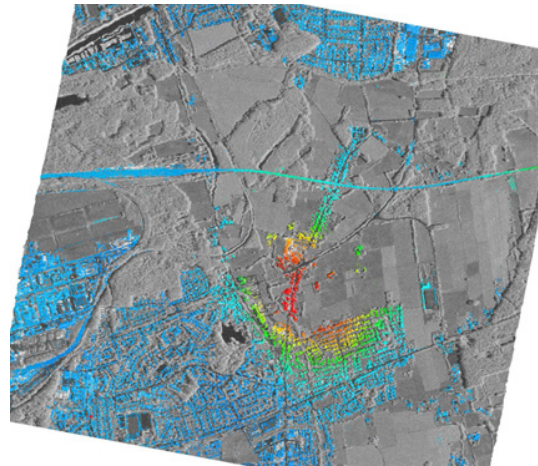


Figure 8. PSI estimated subsidence in TerraSAR-X subset between 11-02-2008 and 21-10-2008

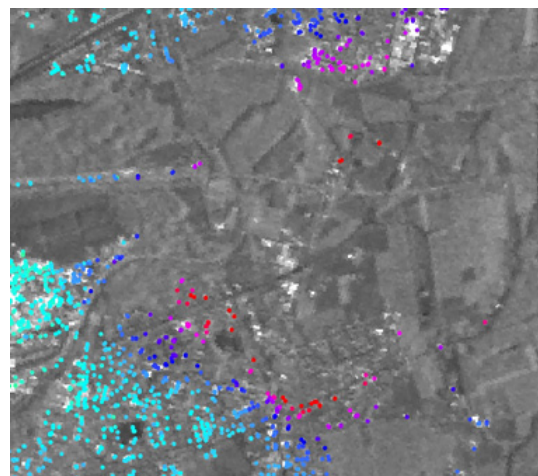


Figure 9. ENVISAT ASAR PSI based subsidence between 18-12-2003 and 11-12-2008 for the same subset as in Figure 8

5. VALIDATION

To validate the interferometric results extensive terrestrial measurements were collected by RAG. SAR displacement results were georeferenced to local *DSK-Ruhr* coordinate system and finally imported into the GIS database "GeoMon" together with the ground truth data. Validation analyses were possible using custom developed graphical GIS tools. More validation details to PALSAR dInSAR see (Walter, 2008) and TerraSAR-X PSI see (Wegmüller, 2008).

5.1 Artificial Corner Reflectors

Six CRs were installed and measured by GPS or levelling during SAR sensor overflights. Differential interferometric phases (low frequency part corrected) of CR peaks detected in SAR intensity images were converted and unwrapped to vertical displacements. The comparison of results of all sensors with terrestrial measurements for one CR is represented in Figure 10. All interferometric analyses were successful, but PALSAR results offered too large time lags. Other CRs showed only very low deformation rates. Under consideration of displacement results of all interferogram combinations (1-2, 2-3, 3-4, 1-3, 1-4, 2-4, ...), best results were reached with TerraSAR-X due to least scatter of deformation results.

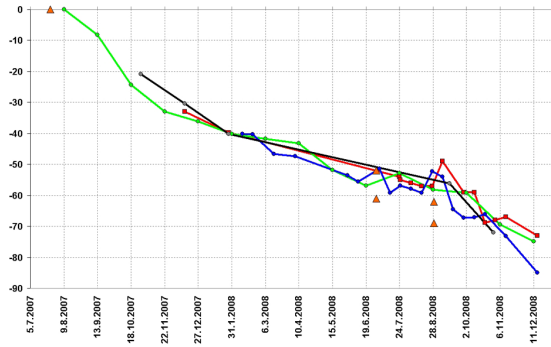


Figure 10. Vertical displacements [mm] of one CR between July 2007 and Dec 2008: GPS (red, orange), TerraSAR-X (blue), ASAR (green), PALSAR (black)

5.2 DInSAR validation

For each detected subsidence trough extensive levelling data were collected every 2-3 months. For each available SAR acquisition a matching levelling date with a time gap smaller than 15 days (PALSAR) or rather 5 days (TerraSAR-X) was searched. 10 profiles along levelling lines could be derived for PALSAR dInSAR results. Figure 11 shows one PALSAR example. In spite of larger time period differences, a good correspondence between the SAR results and the levelling was observed. Overestimation of vertical displacements of ASAR was caused by partly decorrelation after a distance of 700m (see Fig. 11) and resulting phase unwrapping errors.

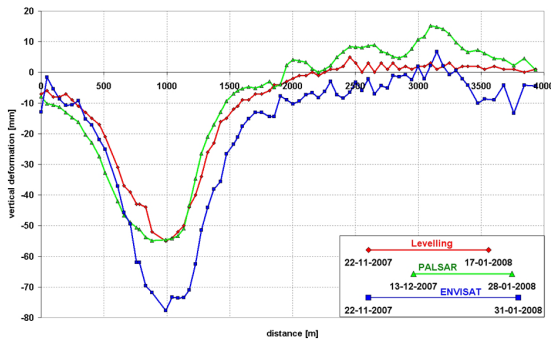


Figure 11. Comparison of levelling (red) with PALSAR dInSAR results (green) and ASAR dInSAR results (blue) [mm]

For validation of TerraSAR-X results reference data for 2-3 month was not sufficient because of fast decorrelation after 11-33 days. An example in Figure 12 shows large gaps after phase unwrapping. For few parts of TerraSAR-X values, ambiguity errors must be corrected manually.

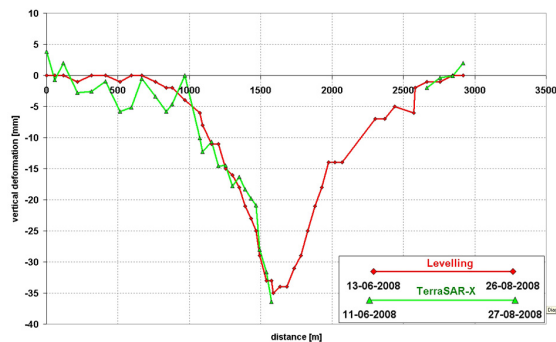


Figure 12. Comparison of levelling (red) with TerraSAR-X dInSAR results (green) [mm]

Differences between levelling and interferometric results were analysed statistically (Tab. 4). Relating to individual levelling lines TerraSAR-X results showed lower variability of mean and standard deviation compared to PALSAR results, because of smaller wavelength. The variation at bisecting line in Figure 13 show clearly better result for TerraSAR-X.

Sensor	Validation n points	Mean [mm]	STDDEV [mm]
PALSAR	466	3.26	13.59
TerraSAR-X	260	0.35	3.94

Table 4. Statistical validation results

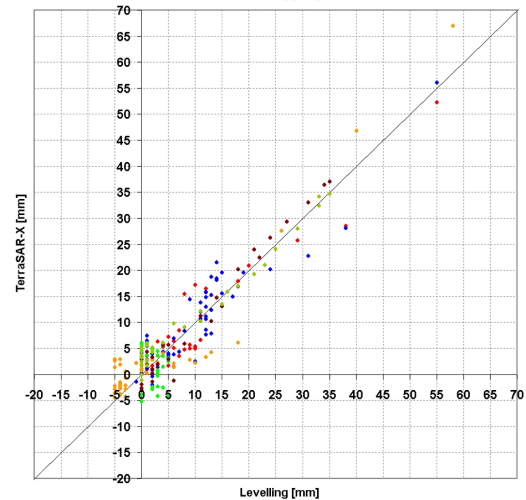
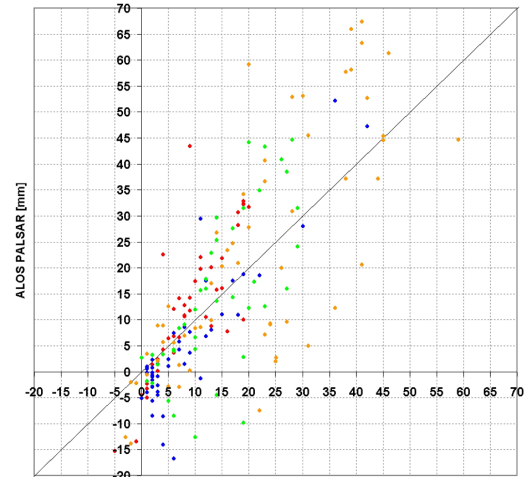


Figure 13. Variation plot for -20mm to 70mm vertical displacements; X-axis: levelling [mm], Y-axis: PALSAR (above), TerraSAR-X (below) results [mm]

5.3 PSI validation

PSI results of TerraSAR-X and ASAR were verified at a few selected levelling points. One or two points of the PSI result in the closer neighbourhood of the levelling points were determined. For these selected locations both the levelling and the PSI values were plotted versus the time. As temporal reference the 4-March 2008 for TerraSAR-X (10-Feb 2005 for ASAR) has been specified, because of the nearly coincident levelling measurements on 5-March 2008 (9-Feb 2005 for ASAR). Thus this vertical displacement for both the levelling and the PSI result was set to 0.0 for this date. Comparisons for two PSI points per sensor are shown in Figure 14 and 15. All

PSI points for both sensors showed good quality for derivation of motions. Small non-linear movements of point 101 were successfully measured with ASAR (Fig. 14). PSI result of point 102 was unsatisfactory, possibly caused by phase unwrapping errors due to large gap in high deformation area and the choice of spatial reference in north east of points.

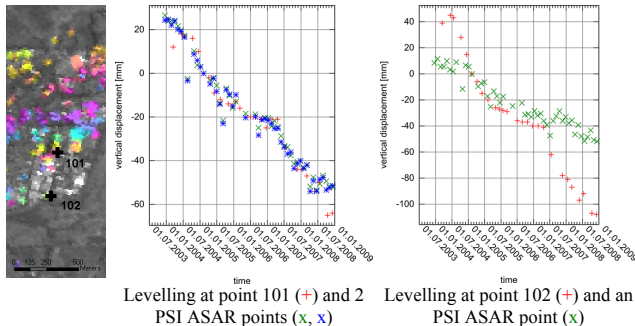


Figure 14. Comparison of levelling and PSI ASAR time series for selected locations

Examples of TerraSAR-X results, shown in Figure 15, confirm the successful application of a multi-reference methodology. The spatial references for the levelling data and for PSI results are located in the nearby neighbourhood. Levelling point 103 is located near an observed maximum subsidence. Here the PSI result indicates around 40cm of subsidence over the 253 days. Overall the PSI result corresponds well to the levelling. There is an initial period with slower subsidence, then a period with fast subsidence (2mm/day) and then towards the end the subsidence slows down again significantly.

One limitation in the reconstruction of the deformation history based on short intervals is that an individual unwrapping error may disturb the entire time series after its occurrence. During the validation work we identified two neighbouring IPTA points near levelling point 104 (Fig. 15) with an offset of about 1.5cm since July 2008. When such errors can be identified we can either reject the inconsistent result or we can correct the phase unwrapping in a post processing.

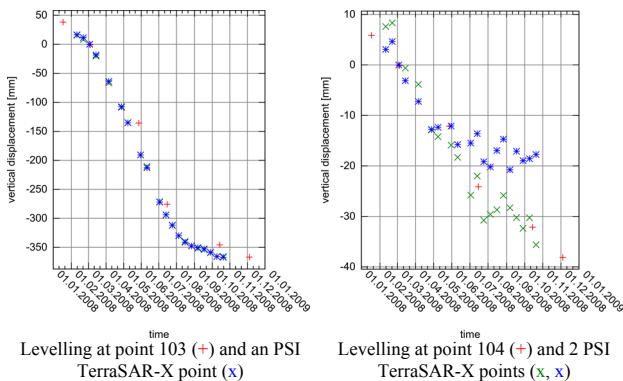


Figure 15. Comparison of levelling and PSI TerraSAR-X time series for selected locations

6. CONCLUSIONS

Results of high-resolution interferometric deformation analysis with ALOS PALSAR and TerraSAR-X in comparison to ENVISAT ASAR were presented.

TerraSAR-X with highest spatial and temporal resolution shows some significant advantages compared to the other sensors. In comparison to ASAR, significantly more PSI points could be

detected with TerraSAR-X especially for urban regions, but also for regions with high deformation gradients and rates. In areas with high deformation gradients TerraSAR-X differential interferograms could be more reliably unwrapped than ASAR differential interferograms. Validation showed very good results for TerraSAR-X with a standard deviation of about 3mm. Disadvantages of TerraSAR-X are fast decorrelation in rural and forest areas and higher influence of atmosphere in interferograms.

The utility of PALSAR data for the monitoring of deformations with high velocity, partly in rural area, was found to be good with average differences of $\pm 13\text{mm}$ between levelling data and interferometric results. In spite of lower sensitivity of the PALSAR sensor to the change of the vegetation cover and atmospheric effects, significant phase unwrapping errors were often observed for areas with low coherence for dInSAR processing. PSI analysis with PALSAR was not possible because of small data stack. In comparison to ASAR sensor, the applicability of L-band was significantly improved for the monitoring of higher subsidence velocities especially in forest areas, because of the longer wavelength and the higher ground resolution. Results show that in most cases C-band interferometry (dInSAR) delivered no deformation results for the test site whereas good results could be achieved with L-band.

7. ACKNOWLEDGEMENTS

This work was supported by: RAG R&D project GEOMON (FE0572-00000) and RFCS2007-Project PRESIDENCE (RFCR-C-2007-0004) of the Research Programme of the Research Fund for Coal and Steel (RFCS). ALOS PALSAR data were provided in the frame of JAXA's RA Program Project 094 "Monitoring of mining induced surface deformation" and of ESA's ALOS ADEN Program Project 3576 "Determination of ground motions in mining areas by interferometric analyses of ALOS data". ENVISAT data are copyright ESA. NEXTMap® Digital Terrain Model was provided by Intermap Technologies Inc., USA as annual license.

8. REFERENCES

Walter, D., U., Wegmüller, V. Spreckels, and W. Busch, 2008. Application and evaluation of ALOS PALSAR data for monitoring of mining induced surface deformations using interferometric techniques. *Proc. of ALOS PI Symposium*, 3-7 Nov 2008, Island of Rhodes, Greece, ESA SP-664 (CD-ROM), H. Lacoste & L. Ouwehand (ed.), ESA Communication Production Office ESTEC, Noordwijk, The Netherlands.

Wegmüller, U., C. Werner, T. Strozzi, and A. Wiesmann, 2004. Multi-temporal interferometric point target analysis. *Analysis of Multi-temporal remote sensing images*, Smits and Bruzzone (ed.), Series in Remote Sensing, Vol. 3, World Scientific (ISBN 981-238-915-61), pp. 136-144, 2004.

Wegmüller, U., D. Walter, V. Spreckels, and C. Werner, 2008. Evaluation of TerraSAR-X DINSAR and IPTA for ground-motion monitoring. *Proc. of The 3rd TerraSAR-X Science Team Meeting*, 25-26 Nov 2008, DLR, Oberpfaffenhofen, Germany.

Werner, C., U. Wegmüller, T. Strozzi, A. Wiesmann, and M. Santoro, 2007. PALSAR Multi-Mode Interferometric Processing. *Proc. First Joint PI Symposium of ALOS data nodes for ALOS Science Program*, 19-23 Nov 2007, Kyoto, Japan.